JRS (2013) Volume 1: Issue 1 | pages 1-14

TDL.ORG TEXAS DIGITAL LIBRARY

Journal of Regulatory Science

http://journalofregulatoryscience.org

PKP PUBLIC KNOWLEDGE PROJECT

Application of Raman spectroscopy for qualitative and quantitative detection of fumonisins in ground maize samples

Kyung-Min Lee [a], Timothy J. Herrman [a, b, *], Christian Nansen [c], Unil Yun [d]

[a] *Office of the Texas State Chemist, Texas A&M AgriLife Research, Texas A&M University System, College Station, TX 77841, USA*

[b] *Texas A&M University, Department of Soil and Crop Sciences, College Station, TX 77843, USA*

[c] *The University of Western Australia, School of Animal Biology, The UWA Institute of Agriculture, Crawley, Perth 6009, Australia*

[d] *Department of Computer Science, School of Electrical and Computer Engineering, Chungbuk National University, CheongJu, Republic of Korea*

ARTICLE INFORMATION

Article History:
Received March 22 2013
Received in revised form
Sept 9 2013
Accepted Oct 8 2013

Keywords:
Fumonisin
Raman spectroscopy
Maize
Food safety
Food security

ABSTRACT

The feasibility of Raman spectroscopy for qualitative and quantitative assessment of fumonisins in ground maize was investigated using the samples with a concentration ranging from 2 to 99 mg/kg. Major Raman bands relevant to an increased level of fumonisins and fumonisin effects on starch molecules were observed in several Raman shift regions. The k-nearest neighbor (KNN) models achieved highest classification accuracies for both training (100%) and independent validation (96–100%) data. Three classification models (k-nearest neighbor, linear discriminant analysis, and partial least squares discriminant analysis) correctly classified fumonisin contaminated samples of >5 mg/kg. All chemometrics models for quantitative determination of fumonisins could explain high levels of variation in spectra data. Multiple linear regression (MLR) and partial least square regression (PLSR) models showed high predictive accuracies and moderate error rates. The statistical results showed no significant difference between LC-MS/MS (liquid chromatography-tandem mass spectrometry) reference and Raman predicted values, implying some models developed have the ability to accurately predict fumonisin levels in ground maize samples for rapid screening and identification of contaminated samples. Thus, the results suggest Raman spectroscopy as a possible fast screening tool for high-throughput analysis of fumonisin contaminated samples to improve food and feed safety.

1. Introduction

Mycotoxin contamination of maize (*Zea mays* L.) kernels caused by *Fusarium* spp is common in most maize production regions of the world and includes fumonisins, deoxynivalinol and zearalenone (Gelderblom et al, 1988). *Fusarium* ear rots may lead to fumonisin contamination produced by *F. moniliforme* and *F. proliferatum* (Miller, 2008). Fumonisin toxicity

* Corresponding author. Department of Soil & Crop Sciences, Texas A&M University, College Station, TX 77841, USA, Tel: (979) 845-1121; fax: (979) 845-1389; E-mail: tjh@otsc.tamu.edu (T. Herrman).

may lead to brain liquefaction in equids, pulmonary edema in swine and is suspected to cause esophageal cancer in humans and neural tube defects in unborn children during pregnancy (Munkvold and Desjardins, 1997). The United States Food and Drug Administration (FDA) and European Commission (EC Commission Regulation 165/2010) released fumonisin advisory levels and maximum tolerance levels, respectively for maize and different maize products. Best practices for preventing infection of maize by *Fusarium* and entry of fumonisin contaminated maize into the food chain are the subject of Codex Alimentarius standards, research, and educational outreach activities (Codex Alimentarius Commission, 2012).

The post-harvest management of maize includes cleaning, milling, and thermal processing and may alleviate fumonisins concentrations in finished products (Bullerman and Bianchini, 2007; Katta et al, 1997; Sydenham et al, 1994). The development of rapid and reliable analytical methods will improve management of fumonisin risk to animal and human health. Fumonisins can be found in visually sound maize kernels, and fungal mass is not always associated with actual fumonisin concentrations. Existing methods widely used for fumonisin analysis include high performance liquid chromatography (HPLC), thin-layer chromatography, gas chromatograph-mass spectrometry (GC-MS), and enzyme-linked immunosorbent assay (ELISA) (Turner et al, 2009). These methods provide accurate and reproducible quantification of fumonisins, but involve complex and time-consuming steps for sample extraction and preparation. These analytical methods are not suitable for a real-time monitoring and a high-throughput screening of a large number of maize samples.

Spectroscopies, such as near-infrared (NIR) and mid-infrared spectroscopy, have been investigated for detection of fumonisins (Dowell et al, 2002; Fernández-Ibañez et al, 2009; Kos et al, 2007; Liu et al, 2009; Pearson et al, 2001; Petterson and Åberg, 2003). The advent of modern inter-ferometric and Fourier transform techniques further improved the spectral accuracy and reproducibility, providing faster and higher resolution of spectrum for characterization of mycotoxins in grains and oilseeds (Fernández-Ibañez et al, 2009; Kos et al, 2002; Peiris et al, 2009; Tripathi and Mishra, 2009). However, spectral interpretation of samples with low mycotoxin concentrations might not be easy because spectrum overlapping and interference from other functional chemical groups generally observed in infrared absorption bands may greatly influence some important bands associated with mycotoxin molecules. In addition, a strong influence by HOH bending absorption of water molecules over the range of infrared wavelengths is likely to distort bands of interest associated with mycotoxin molecules due to residual features of water bands even after subtraction or differentiation (Byler and Susi, 1988).

Raman spectroscopy may overcome some of these constraints that limit the application of spectral-based detection of fumonisin. The principle behind Raman spectroscopy involves irradiation of a substance with a monochromatic light and detection of the scattered light with different frequencies corresponding to the vibrational motions of the molecule (Smith and Dent, 2005). Similar to the infrared spectrum, Raman spectrum provide information about the vibrational transition energy of the molecules. Raman spectroscopy is more sensitive to the symmetrical vibrations of the covalent bonds in nonpolar groups (e.g., C=C and S-S) while infrared spectroscopy better corresponds to asymmetrical vibrations in polar functional groups (e.g., N-H, C=O and O-H) (Skoog et al, 1998). Contrary to infrared spectroscopic techniques, Raman spectroscopy is useful for sample analysis in aqueous conditions due to its insensitivity to water (Colthup et al, 1990). Comparative studies on grain quality classification also showed Raman spectroscopy produces higher spectral resolution and more distinct features than infrared spectroscopic methods (Ma and Phillips, 2002; Sohn et al, 2004).

Raman spectroscopy application in the field of cereal science has been limited, particularly involving the detection of mycotoxins in grains.

Liu et al (2009) use Raman spectroscopy combined with chemometrics to classify low and high level DON-contaminated wheat and barley. Golightly et al (2009) applied surface enhanced Raman spectroscopy (SERS) magnetic bead-based assay to detect aflatoxin B_1 in peanut butter. However, a paucity of information exists involving the application of Raman spectroscopic for the classification and quantification of fumonisin contamination in maize. The objective of this study was to assess the feasibility of Raman spectroscopy combined with chemometrics to develop classification and quantification calibration models for detecting fumonisins in naturally contaminated maize samples.

2. Materials and methods

2.1. Sample preparation

Fumonisin standards (FB1, FB2, and FB3) were obtained from Romer® Labs, Inc.-Biopure (Tullin, Austria). Water and methanol were LC-MS grade, purchased from VWR International, LLC (Bridgeport, NJ). Formic acid was of HPLC grade from Fisher Scientific International, Inc. (Pittsburgh, PA).

Maize samples were obtained from experimental field studies conducted at the Texas A&M AgriLife Research and Extension Center in Lubbock, Texas and from the Office of the Texas State Chemist (OTSC) regulatory samples collected in conformance with the state's plan of work. A total of 100 samples with fumonisin concentrations between 2.0 and 99.0 mg/kg were selected for biochemical and Raman spectral analyses from each of collected sample sets. The selected samples were ground in Retsch® Ultra Centrifugal Mill ZM 200 (Retsch®, Haan, Germany) to pass through a 0.075 mm diameter screen and stored in a polyethylene bottle at 4 °C prior to analysis and between sample measurements. The moisture content of all samples was kept below about 15% to prevent fungal growth in samples. The samples were equilibrated for at least 1 h at room temperature before use.

2.2. Raman spectroscopy

Approximately 5 g of the sample was directly analyzed by Raman spectroscopy (RamanStation™ 400F, Perkin-Elmer®, Beaconsfield, Buckingham-shire, U.K.). All samples were analyzed in quadruplicate. The Raman system was equipped with a near-infrared laser at excitation wavelength of 785 nm and a 256 x 1024 pixel CCD detector. The laser power of 50 mW was used to focus to a 5-mm x 5-mm spot on the sample with exposure times of 2 sec and 5 scans. Spectra data acquisition and analysis were performed using the Spectrum (v. 6.3) software interfaced with the spectroscopy in the Raman shift ranges of 200 to 3500 cm^{-1} at the spectral resolution of 4 cm^{-1}. The spectra from different spots on the sample were co-added to produce a single spectra data. The sample plate was set on an x, y, z-motorized sample holder to automatically align samples and obtain the optimal spectrum.

2.3. Liquid chromatography tandem mass spectrometry (LC-MS/MS) analysis of fumonisins

Fumonisin contaminated samples were analyzed to determine fumonisin B_1 (FB1), fumonisin B_2 (FB2), fumonisin B_3 (FB3) with LC-MS/MS as described in Li et al (2010). Briefly, 50 g of ground maize samples was extracted with 100 mL of methanol/water (70:30, v/v) by shaking for 15 min at 200 rpm. A filtered 25 mL extract was centrifuged at 3000 rpm for 5 min. After centrifugation, the samples with high fumonisin concentrations were additionally diluted with 50% methanol in water. One mL of supernatant aliquot was then spiked with 40 μL of [U-$^{13}C_{34}$]FB_1 solution (250 ng/mL^{-1}) and filtered through a PVDF 0.2 μm syringe filter prior to LC-MS/MS analysis.

The LC-MS/MS system consisted of a Waters® Acquity UPLC coupled to a Quattro Premier XE system equipped with an electrospray interface (ESI) (Waters®, Milford, MA). Chromatographic separation was achieved using a

Waters® Acquity UPLC BEH C18 column (2.1x50 mm, 1.7 um particle size) operated at 50 °C. The mobile phases consisting of A (water with 0.1% formic acid) and B (methanol with 0.1% formic acid) were used at a flow rate of 0.3 mL/min. The gradient conditions were as follows: at 0 min, 50% A : 50% B; at 2.5 min 10% A : 90% B; at 2.6 min 0% A : 100% B; at 3.6 min 50% A: 50% B; at 5.0 min (end), 50% A: 50% B. The mass spectrometer was operated in the positive electrospray ionization (ESI) mode at a cone voltage of 50 V, a source temperature of 140°C, a desolvation temperature of 400°C, and a desolvation gas (nitrogen) flow of 600 L/h. High-purity argon was used as collision gas for multiple reaction monitoring (MRM) at a pressure of 4.7 x 10^{-3} mbar. For the detection of FB1, the precursor ion was m/z 722 and the product ions were selected at m/z 352.4 and 334.4. For FB2 and FB3, the precursor ion was m/z 706 and product ions m/z 318.4 and 336.4. Other parameters of MRM and detailed analytical conditions were described previously (Li et al, 2010).

2.4. Spectral data preprocessing

After background correction by subtracting the Raman scattering noise through the computational process embedded in the Spectrum (v.6.3) software, the spectral data were baseline-corrected and normalized to reduce the systematic variation and the matrix effects. The normalized spectra curve was pretreated by a Savitizky-Golay method with smoothing points of 9 to calculate the first and second derivatives of the spectra. The deconvolution process (Byler and Susi, 1988) for the normalized spectra was also carried out to increase the vertical resolution of unresolved bands.

2.5. Development and validation of fumonisin classification models

The preprocessed spectra data were converted to ASCII format for being utilized by statistical software (SAS® v 9.2, Cary, NC) to perform principal component analysis (PCA) and cluster analysis (CA) (Lee et al, 2005). The chemometric models using k-nearest neighbor (KNN), linear discriminant analysis (LDA), principal component discriminant analysis (PCDA), and partial least squares discriminant analysis (PLSDA) algorithms were developed for classification of non-contaminated and contaminated maize samples using 5 mg/kg fumonisin concentration as threshold. Accordingly, the total number of 100 fumonisin samples was partitioned into 4 different subsets including Group 1 (< 5 mg/kg, considered as fumonisin negative), Group 2 (5–25 mg/kg), Group 3 (25–50 mg/kg), and Group 4 (> 50 mg/kg). Each subset was randomly divided into training (75%) and validation (25%) data set for model development and testing, respectively. The models' performance and accuracy were compared and the best classification model identified based on a correct classification rate and a false negative error. The more detailed procedures for chemometric algorithms applied for this study were described in previous studies (Dowell et al, 2002; Delwiche and Hareland, 2004; Johnson, 1998).

2.6. Development and validation of fumonisin quantification models

The quantification models for fumonisin quantification were developed using multiple linear regression (MLR), partial least squares regression (PLSR), and principal components regression (PCR) algorithms applied to preprocessed spectra data. A total of 100 spectra data were divided into 75% training data for calibration model development and 25% validation data for testing the model. LC-MS/MS reference measurements for fumonisin quantification were compared and correlated with Raman spectra through the developed models. PLSR and PCR algorithms were a spectral decomposition technique that include as much as information possible in the spectra data into the first few factors. The predictive ability of PLSR and PCR models were tested by a cross-validation

method using the leave-one-out option. The optimum number of factors included in the models was determined based on the predicted residual sum of squares (PRESS), and the coefficient of determination (r^2). In MLR analysis, the inclusion and optimum number of wavelengths for the calibration equation were assessed using a stepwise regression and R^2 selection (RSQUARE) methods and comparing statistical parameters including partial r^2 values, partial F-values, and PRESS. The models performance were validated using the root mean standard error of prediction (RMSEP) and correlation coefficient of determination (r^2) using the external data set.

2.7. Statistical analyses

The fumonisin concentrations predicted by chemometrics models were evaluated and compared with the results of reference LC-MS/MS using paired sample t-test, Pearson's correlation coefficients, and ratio of the standard deviation of the reference values to the standard error of cross-validation values (RPD). All data analyses and modeling for classification and quantification of fumonisin contamination were performed using SAS® v 9.1.3 (SAS® Institute, Inc., Cary, NC).

3. Results and discussion

3.1. Spectra data analysis

Fumonisin concentrations measured in the samples for chemometrics models were in the range of 2 to 99 mg/kg, with a mean of 32.5 mg/kg. A positive skewness of the sample set indicates an asymmetrical tail towards higher fumonisin concentrations as evident by a median concentration of 24.5 mg/kg. The training and validation data set yielded similar descriptive statistics for fumonisin concentration. The defined data set should cover the range of fumonisin concentrations found in most raw and processed maize products, and thus is considered suitable to develop the model more useful and representative.

The Raman preprocessed spectra (including baseline correction, normalization, the first and second derivatives, and deconvolution) enhanced characteristic Raman absorption bands, improving classification and predictive accuracy of the models. Preprocessing Raman spectra reduces nonchemical biases (e.g., scattering and particle size effects) to eliminate irrelevant chemical information and to extract only meaningful information (Byler and Susi, 1988; Gowen et al, 2007; Liu et al, 2009). However, it may also amplify spectra that do not reproduce the true band intensities. Fig. 1 shows the difference between non-contaminated and contaminated fumonisin samples resulting from subtracting averaged spectrum of fumonisin negative samples (Group 1) from contaminated ones (Groups 2, 3, and 4). Specific biochemical changes due to fungi attack on maize were more obvious in the difference spectrum than in the absolute spectrum. Raman intensity difference in fumonisin level is often not very visible between low contaminated and non-contaminated samples; however, the spectra may differ in color, chemical, physical, and structural properties of samples.

In this study, Raman intensity differences were distinctive between the four groups of samples over the entire region of Raman spectra. Careful examination of the spectra showed some variations associated with fumonisin concentrations. Fig. 1 shows that Raman intensity of fumonisin samples tended to decrease as fumonisin concentration increased in spectral regions: 428−540 cm^{-1}, 904−948 cm^{-1}, 1012−1176 cm^{-1}, 1264−1476 cm^{-1}, and 1580−1800 cm^{-1}.

The other spectral regions included Raman bands generated by the fungal cellular compounds. The spectral variation within and between groups appeared to be sufficient to produce the models with higher classification and quantification accuracy. Qualitative spectral difference was more observable and visualized in first and second derivative data.

Most significant Raman bands associated with fumonisin effects in maize were observed in the starch regions, around 460−510 cm^{-1} and 1072−1148 cm^{-1} (Table 1). Raman band intensity in the given regions decreased with fumonisin concentration and the individual wavelengths showed higher correlation coefficients, PCA factor loadings (data not shown), and regression coefficients of PLS models (Fig. 2) for fumonisin concentrations than those in other regions. The Raman bands at 480 cm^{-1} and 1084 cm^{-1} are associated with pyranose ring of glucose unit and C-O-H bending in starch, respectively (Kizil et al, 2002; Tu et al, 1979). A strong Raman band at 1128 cm^{-1} corresponds to C-O stretching and C-O-H bending. Distinctive Raman bands appear to reflect increased fumonisin concentrations in maize include 844 cm^{-1} (C-C stretching), 868 cm^{-1} (CH_2 vibration), 1264 cm^{-1} (=C-H symmetric rock), 1488 cm^{-1} (C-H bending), and 1776 cm^{-1} (C=O vibration). These results indicate variations in concentrations of the main component and fumonisins in ground maize samples are measurable by Raman spectral changes.

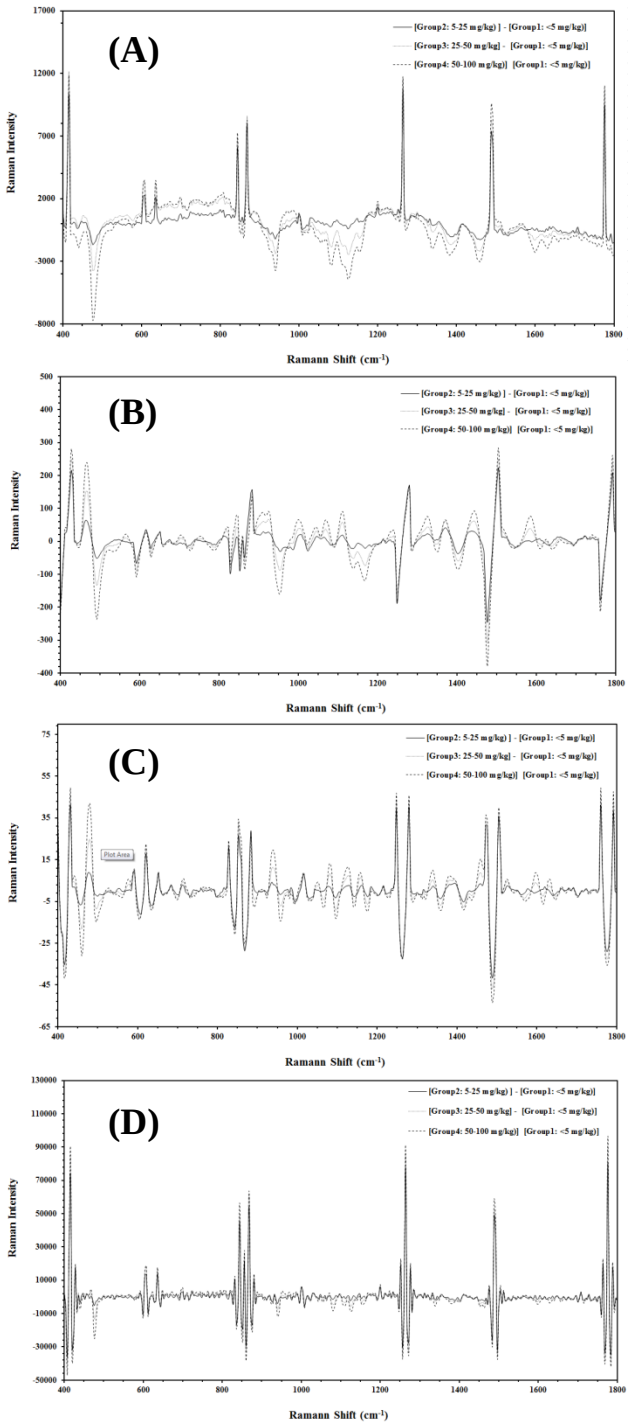

Fig. 1. Averaged Raman subtractive spectra of fumonisin contaminated samples (Groups 2, 3, and 4) from the averaged spectrum of fumonisin negative samples (Group1): (A) normalization; (B). 1st derivative; (C) 2nd derivative; and (D) deconvolution.

3.2. Classification of fumonisin contaminated maize samples

Chemometric models to classify ground maize samples into contaminated and non-contaminated sample groups at different fumonisin concentrations were developed using the four preprocessed spectra data. The performance of the models constructed using the Raman shift region of 400–1800 cm^{-1} is summarized in Table 2. Regardless of preprocessed methods, all three calibration models showed a classification accuracy of 100% by the resubstitution method, in which misclassification rates are usually underestimated (Johnson et al, 1998). The KNN models for all preprocessed data achieved higher classification accuracies for both training and validation data. The PLSDA models showed higher percentages of correct classification rate (97.3–100.0%) for training data while rather lower classification accuracies (64.0–92.0%) were achieved for validation data. The LDA models had higher classification accuracy (96.0–100.0%) for validation data, identical to the KNN models, but a

Table 1
Raman band assignments for Raman spectra of fumonisin contaminated samples.

Raman shift (cm^{-1})	Band assignments	Reference[a]
440	Skeletal modes of pyranose ring of glucose unit in starch	6, 7, 8, 13
480	C-O vibration in starch	6, 7, 8
760	C-C stretching in starch	7, 14
844	C-C stretching	1
860	CH and CH_2 deformation in starch	4, 7, 8
868	C-O-C skeletal mode	11
940	Skeletal mode vibrations of α1-4 glycosidic linkage in starch	4, 7, 8, 13
1084	C-O-H bending in starch	6, 7
1128	C-O stretching, C-O-H bending in starch	7, 10
1264	=C-H symmetric rock	5
1268	CH_2OH (side chain) related mode in starch	7,10
1384	CH_2 scissoring, C-H and C-O-H deformation in starch	6, 7
1460	CH_2 bending in starch	4, 6, 7
1488	C-H bending	2, 3, 9
1776	C=O vibration	2, 9, 12

[a]Corresponding references for band assignments are as follows: 1. Arp et al, 2001; 2. Baeten et al, 1998; 3. Boca et al, 2012; 4. Cael et al, 1973; 5. Howell et al, 2001; 6. Kizil and Irudayaraj, 2007; 7. Kizil et al, 2002; 8. Lee et al, 2010; 9. Móricz et al, 2008; 10. Santha et al, 1990; 11. Schulz and Baranska, 2007; 12. Taddei et al, 2001; 13. Tu et al, 1979; 14. Wu et al, 2012.

misclassification rate for training data set was higher than the other chemometrics models.

In the KNN analysis, classification accuracies of the models became stable when the number of neighbors exceeded five. The model for normalized data achieved a classification accuracy of 100% for training data set, with corresponding validation classification accuracy of 100%. The rate of correct classification of the models for other preprocessed data was 100% for training data set, with 96% classification accuracy for validation data set. In these models, only one sample was incorrectly assigned to the group with fumonisin concentrations close to the group where the sample originates. The level of accuracy obtained with KNN models using Raman spectra is comparable with or superior to that reported in previous studies with near infrared spectrometer (Dowell et al, 2002; Pearson et al, 2004). When the developed KNN models were applied to validation data set, none of the fumonisin contaminated samples were misclassified as fumonisin negative. This was also observed in LDA and PLSDA models although they displayed lower classification accuracy than KNN models (Table 2). This zero misclassification of fumonisin positive samples as negative by Raman technique is vital for use as a high-throughput test for screening samples, which may greatly help manage a risk of crop contamination and human and animal exposure to fumonisins.

As mentioned earlier, LDA and PLSDA models exhibited the opposite trend in the level of classification accuracy for training and validation data set (Table 2). LDA models for the preprocessed data resulted in moderate classification accuracies for training data set and similar validation accuracy to the KNN models for validation data set. The PLSDA models could correctly classify fumonisin positive and negative samples with >97.3% accuracy for training data set. However, when the models were applied to validation data set, the classification accuracy dropped significantly, particularly with 2^{nd} derivative data (64%). Difference in classification accuracy between training and validation data set may be in part attributed to the

Table 2
Correct classification rate of fumonisin contamination groups at different concentration using chemometric models for different preprocessed spectral data[a]

Preprocessing method	KNN			LDA			PLSDA		
	Training (%)	Validation (%)	False negative error (%) [b]	Training (%)	Validation (%)	False negative error (%)	Training (%)	Validation (%)	False negative error (%)
Normalization	100.0	100.0	0.0	92.0	100.0	0.0	97.3	92.0	0.0
1st derivative	100.0	96.0	0.0	81.3	96.0	0.0	97.3	92.0	0.0
2nd derivative	100.0	96.0	0.0	92.0	96.0	0.0	100.0	64.0	0.0
Deconvolution	100.0	96.0	0.0	92.0	96.0	0.0	100.0	80.0	0.0

[a] KNN, *k*-nearest neighbor; LDA, linear discriminant analysis; PLSDA, partial least squares discriminant analysis.;
[b] A false negative error (%) was defined as the failure of the model to classify fumonisin contaminated samples as negative (Group 1).

fact that in PLSDA model, the sample is assigned to one of four groups for their predicted fumonisin content by PLS regression (Reeves and Delwiche, 2008). In other words, the PLSDA was not developed for classification purposes (Pearson et al, 2001). Compared to other models, the PCDA models displayed a lower accuracy range of 86.7–90.7% for training data set, 16–76% accuracy for validation data set (data not shown) and many contaminated samples were misclassified as fumonisin negative. High misclassification rate of the PCDA models typically results from spectral similarity leading to poor separation of samples in principal component scores and through the interference of Raman bands for fumonisins by other chemical groups.

3.3. Quantification of fumonisin in maize samples

Multivariate data analysis provides a powerful tool for extraction of meaningful information to overcome some limitations in univariate techniques and to detect a small difference in spectra between contaminated and non-contaminated samples and among contaminated samples with mycotoxins (Abramović et al, 2007; Kos et al, 2007; Liu et al, 2009). In a multivariate system, single spectra with high correlation coefficients with the reference data may be grouped and analyzed together. For the present study, three chemometrics (MLR, PLSR, and PCR) for all preprocessed spectra data at the Raman shift range of 400−1800 cm^{-1} were used to develop calibration models for fumonisin quantification to explain the relationships between fumonisin concentrations and Raman spectra. The results of chemometric models and statistical analysis applied to training and validation data are presented in Tables 3 and 4. Some differences in the results were noticed among chemometrics models, and among preprocessed spectra data within each chemometric method. Although PLSR models performed slightly better than MLR models in predicting fumonisin concentration of the training data set, both PLSR and MLR models generally showed comparable results. Compared to these two chemometrics, the results of PCR models were not as good and displayed the least predictive accuracy.

All MLR and PLSR models could explain >90% of variation in the preprocessed spectra data in both training and validation data, except for the models for 2nd derivative preprocessed data. The PCR models could predict the variation range of 80−86% in the preprocessed data (Table 3). The MLR and PLSR models also displayed low error rates compared to the PCR models. However, the differences in prediction errors between training

and validation data set were larger in MLR and PLSR models than in PCR models, implying that MLR and PLSR models can be more affected by small spectral variations irrelevant to changes in the compositions of samples (Kim et al, 2008). MLR and PLSR models also produced stronger correlation coefficients with LC-MS/MS values and higher RPD values (Table 4), indicating better predictive performance than PCR models.

The MLR models included the optimum wavelengths selected by testing all possible combinations of wavelengths and removing collinearity among highly correlated wavelengths to produce the best results (Broadhurst et al, 1996). According to the statistical results of slope, coefficients of determination (r^2), RMSEC, and RMSEP in Table 3, normalized and deconvolution preprocessing appeared to be helpful in improving performance of the MLR models. Linear regressions of the MLR models for training data set showed high r^2 and moderate error rate (RMSEC) values in the ranges of 0.856–0.932 and 7.177–8.782 mg/kg, respectively. When the models were further applied to the validation data set to estimate the overall predictive accuracy, the models yielded similar performance and accuracy with acceptable levels of r^2 (0.856–0.915) and slightly higher error rate (7.745–10.380 mg/kg). The slopes of the linear regressions were in the range of 0.884–0.977 for training and validation data set, indicating the acceptable quality of the regression and the reliability of some selected models. The MLR models also showed a good linear correlation (r = 0.925–0.957) (Table 4), implying a good agreement between Raman predicted and reference LC-MS/MS values. Selected wavelengths in the MLR models indicated the most influential wavelengths are associated with starch molecules. These observations indicate that a slight improvement of current MLR models by optimizing instrumental and measurement conditions may allow for accurately predicting low and high fumonisin levels in ground maize samples.

The prediction results of PLSR models are displayed in Tables 3 and 4. As in PCR, PLSR uses a few factors including information from all wavelengths in the spectra to predict a target analyte of interest (Cramer, 1993). This feature allows one to correlate Raman spectra with fumonisin concentration even when visual difference in the spectra is not significant among fumonisin contaminated samples. PLSR require fewer factors and more powerful than PCR to produce comparable results (Osborne et al, 1993). The optimum number of factors is determined by calculating the predicted residual error sum of squares (PRESS) using leave-one-out cross validation method for training data set. The calibration models yielded relatively higher r^2 values (0.930–0.975) and low error rate (RMSEC: 5.016–7.165 mg/kg), with a linear regression slope in the range of 0.936–0.977, showing a good correlation between actual and predicted values. The calibration models applied to the validation data set produced a comparable quality of regression with slope range of 0.952–0.998, but a rather higher error rate (RMSEP: 8.231–9.607 mg/kg). A high positive correlation (r > 0.929) plots of absolute values of correlation coefficients versus wavelengths for the PLSR models for normalized and 1^{st} derivative data. This figure can provide additional information on particular spectral sub-ranges and peaks. Wavelengths with a larger coefficient value can contribute more to a calibration model (Balcerowska et al, 2009).

In Fig. 2, larger values in spectral regions and peaks appeared to be associated with starch and fumonisin molecules, which is consistent with the findings described above. The PCR calibration models applied to validation data set displayed less predicting ability (r^2 = 0.829–0.860 and RMSEP = 10.274–11.251 mg/kg) to measure fumonisin content compared to MLR and PLRS models (Table 3).

Predicted values of three chemometric models were statistically compared with reference LC-MS/MS data with paired sample t-test using validation data set (Table 4). Statistical results indicated there were no significant differences between the means of Raman and reference LC-MS/MS method although predictive accuracy and

Table 3
Predictive accuracy and error rates of three chemometric models fitted to preprocessed spectra data in predicting fumonisin concentrations in ground maize samples.

Chemometrics	Preprocessing method	Training data			Validation data		
		RMSEC (mg/kg)[a]	Slope	r^{2c}	RMSEP (mg/kg)[b]	Slope	r^{2c}
MLR	Normalization	8.126	0.912	0.912	8.624	0.977	0.903
	1st derivative	8.782	0.884	0.901	7.745	0.926	0.915
	2nd derivative	8.101	0.912	0.856	10.380	0.916	0.856
	Deconvolution	7.177	0.932	0.932	9.017	0.899	0.903
PCR	Normalization	11.336	0.830	0.830	10.274	0.913	0.859
	1st derivative	10.445	0.852	0.842	10.426	0.858	0.860
	2nd derivative	11.686	0.803	0.803	11.251	0.836	0.829
	Deconvolution	11.132	0.834	0.836	10.991	0.885	0.838
PLSR	Normalization	5.832	0.955	0.955	8.730	0.967	0.905
	1st derivative	7.165	0.937	0.930	8.231	0.954	0.910
	2nd derivative	5.016	0.977	0.965	9.607	0.952	0.864
	Deconvolution	6.977	0.936	0.936	8.729	0.998	0.900

[a] RMSEC: root-mean-square error of calibration.; [b] RMSEP: root-mean-square error of prediction .; [c] r^2: correlation coefficient of determination.

Table 4
Statistical results of paired sample t-test for difference between reference LC-MS/MS and Raman predicted values

Parameters	MLR				PCR				PLSR			
	Norm[a]	1 D[b]	2 D[c]	Decon[d]	Norm	1 D	2 D	Decon	Norm	1 D	2 D	Decon
Paired differences												
Mean	-1.79	-0.70	-2.83	-2.45	-2.34	-3.35	-2.03	-3.06	-2.89	-1.73	-2.64	-1.89
Std deviation	8.53	7.80	9.98	8.77	10.25	9.98	11.06	10.61	8.22	8.24	8.89	8.13
Std error mean	1.27	1.14	1.49	1.29	1.54	1.47	1.65	1.58	1.50	1.23	1.32	1.24
r^e	0.950	0.957	0.925	0.950	0.927	0.928	0.910	0.916	0.952	0.954	0.929	0.948
t-value	1.579	0.611	1.924	1.898	1.492	2.273	1.246	2.083	2.364	1.410	1.703	1.610
Sig (2-tailed)	0.122	0.544	0.061	0.064	0.143	0.028	0.219	0.043	0.022	0.165	0.096	0.115
RPD[f]	3.082	3.449	2.519	3.123	2.596	2.562	2.399	2.393	3.504	3.264	2.771	2.947

[a] Norm: normalized data. [b]1D: 1st derivative data. [c]2D: 2nd derivative data. [d]Decon: deconvolution data. [e]r: Pearson's correlation coefficient. [f]RPD: ratio of the standard deviation of the reference values to the standard error of cross-validation values.

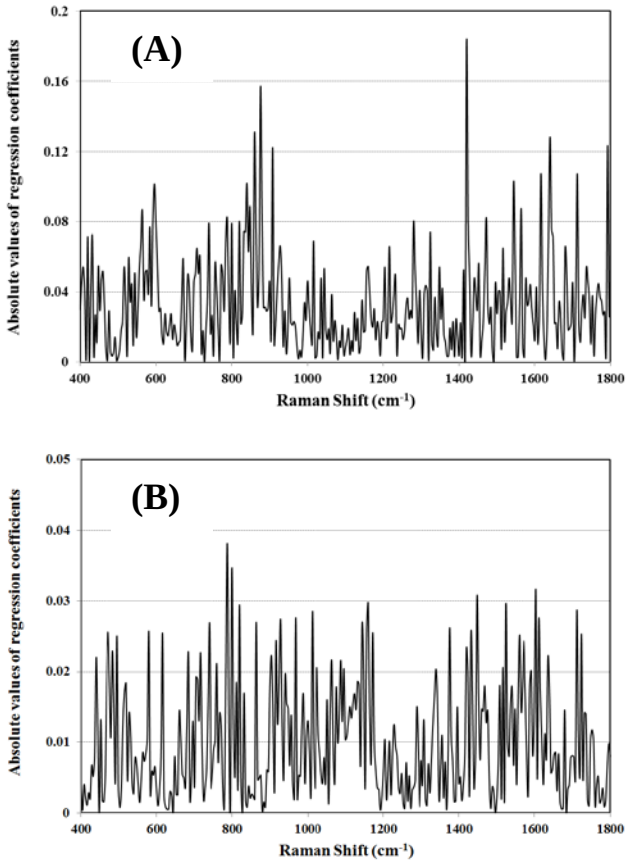

Fig. 2. Absolute regression coefficients of PLSR models for normalized (A) and deconvolution data (B).

error were slightly different among chemometrics and preprocessed methods within each chemometric method. As expected, standard errors of MLR and PLSR models were slightly lower than those of PCR models. The significance levels of *p*-value and correlation coefficients close to one indicated the models yielded generally comparable results to LC-MS/MS method at levels tested in this work. RPD values calculated by standardizing the RMSEP against standard deviation of the reference data in the validation data set showed the ranges of 2.519 to 3.449, 2.393 to 2.596, and 2.771 to 3.504, for MLR, PCR, and PLSR models, respectively. These RPD value ranges indicate that the models have a high predictive ability to differentiate between lower and higher fumonisin contaminated samples for screening (Armstrong et al, 2007; Williams, 2001). These findings seem to imply that the developed models can readily predict fumonisin concentration and are comparable to conventional time-consuming chemical methods for fumonisin analysis within a specific fumonisin concentration range.

In conclusion, the proposed Raman spectroscopic method combined with chemometrics has demonstrated its potential and challenges as alternative rapid and non-destructive technique for qualitative and quantitative determination of fumonisin levels in ground maize for screening fumonisin contaminated samples. Classification and quantification models showed a good predictive performance with a high overall accuracy and moderate error rate, offering significantly reduced risk of misclassification of fumonisin contaminated maize samples as fumonisin negative. These features may be desirable for real-time monitoring of critical performance attributes in controlling feed and food manufacturing processes utilizing contaminated maize as major raw or starting materials. Despite anticipating several difficulties and constraints in using this technique for fumonisin analysis, such as inaccuracy in the low concentration range and low-to-moderate repeatability and reproducibility of spectra, there may be numerous opportunities to improve the accuracy and precision of Raman spectroscopy measurements. The calibration models obtained from this study would be more stable and practically applicable by continuing to analyze maize samples with diverse genetic and environmental backgrounds and fumonisin levels. Raman spectroscopy as an easy, rapid, and inexpensive screening system for fumonisins and other mycotoxins can be a valuable adjunct tool for quality control of grains and oilseeds throughout the entire marketing chain to improve the safety of feed and food products supplied to consumers.

Declaration of conflicting interest

The authors declare that there is no conflict of interest.

Acknowledgements

The authors wish to acknowledge financial support by the Andersons Endowment administered through the Ohio Agricultural Research and Development Center of The Ohio State University.

References

Abramović, B., Jajić, I., Abramović, B., Cosić, J., & Jurić, V. (2007). Detection of deoxynivalenol in wheat by Fourier transform infrared spectroscopy. *Acta Chimica Slovenica*, 54, 859–867.

Armstrong, P.R., Lingenfelser, J.E., & McKinney, L. (2007). The effect of moisture content on determining corn hardness from grinding time, grinding energy, and near-infrared spectroscopy. *Applied Engineering in Agriculture*, 23, 793–799.

Arp, Z., Autrey, D., Laane, J., Overman, S.A., & Thomas, G.J., Jr. (2001). Tyrosine Raman signatures of the filamentous virus Ff are diagnostic of non-hydrogen-bonded phenoxyls: Demonstration by Raman and infrared spectroscopy of p-cresol vapor. *Biochemistry*, 40, 2522–2529.

Baeten, V., Hourant, P., Morales, M., & Aparicio, R. (1998). Oil and fat classification by FT-Raman spectroscopy. *Journal of Agricultural Food Chemistry*, 46, 2638–2646.

Balcerowska, G., Siuda, R., Skrzypczak, J., Lukanowski, A., & Sadowski, C. (2009). Effect of particle size and spectral sub-range within the UV-VIS-NIR range using diffuse reflectance spectra on multivariate models in evaluating the severity of fusariosis in ground wheat. *Food Additives and Contaminants*, 26, 726–732.

Boca, S., Rugina, D., Pintea, A., Leopold, N., & Astilean, S. (2012). Designing gold nanoparticle-ensembles as surface enhanced Raman scattering tags inside human retinal cells. *Journal of Nanotechnology*, 2012,1–10.

Broadhurst, D., Goodacre, R., Jones, A., Rowland, J.J., & Kell, D.B. (1997). Genetic algorithms as a method for variable selection in multiple linear regression and partial least squares regression, with applications to pyrolysis mass spectrometry. *Analytica Chimica Acta*, 348, 71−86.

Bullerman, L. B., & Bianchini, A. (2007). Stability of mycotoxins during food processing. *International Journal of Food Microbiology*, 119, 140–146.

Byler, D.M.; & Susi, H. (1988). Application of computerized infrared and Raman spectroscopy to conformation studies of casein and other food proteins. *Journal of Industrial Microbiology*, 3, 73–88.

Cael, J. J., Koenig, J. L., & Blackwell, J. (1973). Infrared and Raman spectroscopy of carbohydrates. Part III: Raman spectra of the polymorphic forms of amylose. *Carbohydrate Research*, 29, 123-134.

Codex Alimentarius Commission (2012). Joint FAO/WHO Food Standards Programme Codex Committee on Contaminants in Foods, Discussion paper on proposed draftmaximum levels for fumonisins in maize and maize-products and associated sampling plans, European Union, Maastricht, The Netherlands.

Colthup, N. B., Daly, L. H., & Wiberley, S. E. (1990). Introduction to Infrared and Raman Spectroscopy (3rd ed.). San Diego, CA: Academic Press.

Cramer, R.D., III., (1993). Partial least squares (PLS): Its strengths and limitations. *Perspectives in Drug Discovery and Design*. 1, 269–278.

Delwiche, S.R., & Hareland, G.A. (2004). Detection of scab-damaged hard red spring wheat kernels by Near-Infrared Reflectance. *Cereal Chemistry*, 81, 643–649.

Dowell, F.E., Pearson, T.C., Maghirang, E.B., Xie, F., & Wicklow, D.T. (2002). Reflectance and transmittance spectroscopy applied to detecting fumonisin in single corn kernels infected with *Fusarium verticillioides*. *Cereal Chemistry*. 79, 222-226.

Fernández-Ibañez, V., Soldado, A., Martínez-Fernández, A., & de la Roza-Delgado, B. (2009). Application of near infrared spectroscopy for rapid detection of aflatoxin B_1 in maize and barely as analytical quality assessment. *Food Chemistry*, 113, 629–6340.

Gelderblom, W. C. A., Jaskiewicz, K., Marasas, W. F. O., Thiel, P. G., Horak, R. N., Vlegger, R., & Kriek, N.P. (1988). Fumonisins – novel mycotoxins with cancer promoting activity produced by *Fusarium moniliforme*. *Applied and Environmental Microbiology*, 54, 1806–1811.

Golightly, R.S., Doering, W.E., & Natan, M.J. (2009). Surface-enhanced Raman spectroscopy and homeland security: a perfect match?. *Nano*, 3, 2859–2869.

Gowen, A.A., O'Donnella, C.P., Cullenb, P.J., Downeyc, G., & Frias, J.M. (2007). Hyperspectral imaging e an emerging process analytical tool for food quality and safety control. *Trends in Food Science & Technology*, 18, 590–598.

Howell, N.Z., Herman, H., & Li-Chan, E.C.Y. (2001). Elucidation of protein-lipid Interactions in a lysozyme-corn oil system by Fourier transform Raman spectroscopy. *Journal of Agricultural Food Chemistry*, 49, 1529–1533.

Johnson, D. E. (1998). Discriminant analysis. In D. E. Johnson (Ed.), *Applied Multivariate Methods for Data Analysts* (pp. 217−285). California: Duxbury Press.

Katta, S.K., Cagampang, A.E., Jackson, L.S., & Bullerman, L.B. (1997). Distribution of Fusarium molds and fumonisins in dry-milled corn fractions. *Cereal Chemistry*. 74, 858–863.

Kim, J., Hwang, J., & Chung, H. (2008). Comparison of near-infrared and Raman spectroscopy for on-line monitoring of etchant solutions directly through a Teflon tube. *Analytica Chimica Acta*. 629, 119−127.

Kizil, R. Irudayaraj, J., & Seetharaman, K. (2002). Characterization of irradiated starches by using FT-Raman and FTIR spectroscopy. *Journal of Agricultural Food Chemistry*, 50, 3912−3918.

Kizil, R., & Irudayaraj, J. (2007). Rapid evaluation and discrimination of γ -irradiated carbohydrates using FT-Raman spectroscopy and canonical discriminant analysis. *Journal of the Science of Food and Agriculture*. 87, 1244–1251.

Kos, G., Lohninger, H., & Krska, R. (2002). Fourier transform mid-infrared spectroscopy with attenuated total reflection (FT-IR/ATR) as a tool for the detection of *Fusarium* on maize. *Vibrational Spectroscopy*, 29, 115–119.

Kos, G., Lohninger, H., Mizaikoff, B., & Krska, R. (2007). Optimisation of a sample preparation procedure for the screening of fungal infection and assessment of deoxynivalenol content in maize using mid-infrared attenuated total reflection spectroscopy. *Food Additives and Contaminants*, 24, 721–729.

Lee, K.M., Armstrong, P.R., Thomasson, A., Sui, R., Casada, M., & Herrman, T. J. (2010). Development and characterization of food-grade tracers for the global grain tracing and recall system. *Journal of Agricultural Food Chemistry*, 58, 10945–10957.

Lee, K.M., Herrman, T.J., Lingenfelser, J., & Jackson, D.S. (2005). Classification and prediction of maize hardness-associated properties by using multivariate statistical analyses. *Journal of Cereal Science*, 41, 85**–**93.

Li, W., Herrman, T.J., & Dai, S.Y. (2010). Rapid determination of fumonisins in corn-based products by liquid chromatography-tandem mass spectrometry, *Journal of AOAC International*, 93, 1472–1481.

Liu, Y., Delwiche, S.R., & Dong, Y. (2009). Feasibility of FT-Raman spectroscopy for rapid screening for DON toxin in ground wheat and barley. *Food Additives and Contaminants*, 26, 1396–1401.

Ma, C.Y., & Phillips, D.L. (2002). FT-Raman spectroscopy and its applications in cereal science. *Cereal Chemistry*. 79, 171–177.

Miller, J.D. (2008). Mycotoxins in small grains and maize: Old problems, new challenges. *Food Additives and Contaminants*, 25, 219–230.

Móricz, Á.M., Horváth, E., Ott, P.G., & Tyihák, E. (2008). Raman spectroscopic evaluation of the influence of Pseudomonas bacteria on aflatoxin B_1 in the BioArena Complex bioautographic system. *Journal of Raman Spectroscopy*, 39, 1332−1337.

Munkvold, G. P., & Desjardins, A. E. (1997). Fumonisins in maize: can we reduce their occurrence? *Plant Disease*. 81, 556–565.

Osborne, B.G., Fearn, T., & Hindle, P.H. (1993). Near infrared calibration II. In B.G. Osborne, T. Fearn, P.H. Hindle, & P.T. Hindle (Eds.), *Practical NIR Spectroscopy with Applications in Food and Beverage Analysis* (pp. 121−144). Harlow, UK: Longman Scientific & Technical.

Pearson, T. C., Wicklow, D. T., Maghirang, F., Xie, F. E., & Dowell, F.E. (2001). Detecting aflatoxin in single corn kernels by transmit and reflectance spectroscopy. Transactions of ASAE, 44, 1247–1254.

Pearson, T.C., Wicklow, D.T., & Pasikatan, M.C. (2004). Reduction of aflatoxin and fumonisin contamination in yellow corn by high-speed dual-wavelength sorting. *Cereal Chemistry*, 81, 490–498.

Peiris, K.H.S., Pumphrey, M.O., & Dowell, F.E. (2009). NIR absorbance characteristics of deoxynivalenol and of sound and Fusarium-damaged wheat kernels. *Journal of Near Infrared Spectroscopy*, 17, 213–221.

Petterson, H. & Åberg, L. (2003). Near-infrared spectroscopy for determination of mycotoxins in cereals. *Food Control*, 14, 229–232.

Reeves, J.B., & Delwiche, S.R. (2008). SAS partial least squares for discriminant analysis. *Journal of Near Infrared Spectroscopy*, 16, 31–38.

Santha, N., Sudha, K. G., Vijaykumari, K. P., Nayar, V. U., & Moorthy, S. N. (1990). Raman and Infrared spectra of starch samples of sweet potato and cassava. *Proceedings of the Indian Academy of Sciences* (*Chemical Sciences*), 102, 705−712.

Schulz, H., & Baranska, M. (2007). Identification and quantification of valuable plant substances by IR and Raman spectroscopy. *Vibrational Spectroscopy*, 43, 13–25.

Skoog, D. A., Holler, F. J., & Nieman, T. A. (1998). Principles of Instrumental Analysis. Philadelphia, PA: Harcourt Brace College Publishers.

Smith, E., & Dent, G. (2005). Introduction, basic theory and principles. In E. Smith, & G. Dent. *Modern Raman spectroscopy-A practical approach* (pp.1–21). West Sussex, UK: John Wiley & Sons Ltd.

Sohn, M., Himmelsbach, D.S., & Barton, F.E. (2004). A comparative study of Fourier transform Raman and NIR spectroscopic methods for assessment of protein and apparent amylose in rice. *Cereal Chemistry*, 81, 429–433.

Sydenham, E.W., Van der Westhuizen, L., Stockenström, S., Shepard, G.S., & Thiel, P.G. (1994). Fumonisin-contaminated maize: physical treatment for the partial decontamination of bulk shipments. *Food Additives and Contaminants*, 11, 25–32.

Taddei, P., Tinti, A., & Fini, G. (2001). Vibrational spectroscopy of polymeric biomaterials. *Journal of Raman Spectroscopy*, 32, 619–629

Tripathi, S., & Mishra, H.N. (2009). A rapid FT_NIR method for estimation of aflatoxin B_1 in red chili powder. *Food Control*, 20, 840−846.

Tu, A. T., Lee, J., & Milanovich, F. P. (1979). Laser-Raman spectroscopic study of cyclohexaamylose and related compounds; spectral analysis and structural implications. *Carbohydrate Research*, 76, 239-244.

Turner, N.W., Subrahmanyam, S., & Piletsky, S.A. (2009). Analytical methods for determination of mycotoxins: A review. *Analytica Chimica Acta*, 632, 168–180.

Williams, P. C. (2001). Implementation of near-infrared technology. In P.C. Williams, & K. Norris (Eds.) *Near-Infrared Technology in the Agricultural and Food Industries* (pp. 145−169). Minnesota: American Association of Cereal Chemists.

Wu, X., Gao, S., Wang, J.S., Wang, H., Huang, Y.W., & Zhao, Y. (2012). The surface-enhanced Raman spectra of aflatoxins: spectral analysis, density functional theory calculation, detection and differentiation. *Analyst*, 137, 4226−4234.